The Effect of High Energy Milling on the Solid State Synthesis of $MnFe_2O_4$ from Mixtures of $MnO-Fe_2O_3$ and $Mn_3O_4-Fe_2O_3$

V. Berbenni[a], A. Marini[a], A. Profumo[b], and L. Cucca[b]

[a] CSGI – CNR IENI – Dipartimento di Chimica Fisica dell'Università di Pavia Via Taramelli 16, 27100 Pavia, Italy
[b] Dipartimento di Chimica Generale dell'Università di Pavia Via Taramelli 12, 27100 Pavia, Italy

Reprint requests to Dr. V. Berbenni. Fax: 0039-0382-507575. E-mail: berbenni@matsci.unipv.it

Z. Naturforsch. **58b,** 415–422 (2003); received January 30, 2003

A thermal treatment at 900 °C (under nitrogen) of a milled mixture $MnO-Fe_2O_3$ yields $MnFe_2O_4$ mainly as the product of the reaction between Mn_3O_4 (produced by ball milling) and Fe_2O_3. Under the same experimental conditions but starting from an unmilled $MnO-Fe_2O_3$ mixture, the formation of $MnFe_2O_4$ is only partial and occurs through Mn_3O_4 (formed by oxidation of MnO). The same thermal treatment (900 °C under nitrogen) of a milled $Mn_3O_4-Fe_2O_3$ mixture yields $MnFe_2O_4$ mainly as the product of the reaction between Mn_3O_4 and Mn_2O_3/MnO_2 (the higher Mn oxides being produced by ball milling) and Fe_2O_3. The effect of high energy milling is more pronounced in the case of the $Mn_3O_4-Fe_2O_3$ system since no $MnFe_2O_4$ formation is observed when starting from a physical mixture.

Key words: Mechanical Activation, Manganese Ferrite, Thermogravimetric Analysis

Introduction

The spinel ferrites [general formula $M^{II}(Fe^{III})_2O_4$] find applications in both technological and catalytic fields [1] . In particular manganese ferrite belongs to a group of technically important materials in the electrical and electronic industry. As starting materials for manufacturing ceramics, fine-grained, pure ferrite powders with well defined chemical compositions are necessary. To prepare such powders a number of wet routes such as co-precipitation of hydroxides [2], carbonates [3] and oxalates [4] or freeze-drying of mixed carboxylates [5] have been proposed. These chemical precursor methods are deemed to have an advantage over the conventional, high temperature solid state synthesis, which suffers of some drawbacks such as non-homogeneity, large particle size (hence low surface area) and poor sinterability. Dreraz *et al.* [6] carried out solid state reactions between manganese(II) carbonate and iron(III) oxide. They succeeded in obtaining $MnFe_2O_4$ at temperatures starting from 900 °C and demonstrated that Li_2O acts as a catalyst in $MnFe_2O_4$ formation. This notwithstanding, they concluded that complete conversion from Mn_2O_3 (produced from $MnCO_3$ decomposition) and Fe_2O_3 to $MnFe_2O_4$ requires prolonged heating at T > 1100 °C.

In recents years we have undertaken a study of the influence of high-energy ball milling on solid state synthesis of ferrites of Li [7], Ba [8] and Sr [9]. It has been shown that, starting from mechanically activated mixtures of oxides/carbonates/oxalates, the solid state synthesis takes place at sensibly lower temperatures. This should allow to obtain the desired product with smaller particle sizes. Besides, the solid state reaction starting from a milled reacting mixture very often leads to final products through a single stage process. The present work reports the results obtained in the study of the solid state synthesis of $MnFe_2O_4$ starting from mechanically activated mixtures of hematite with manganese oxides (MnO, Mn_3O_4). Thermogravimetric analysis (TGA), differential scanning calorimetry (DSC), X-ray powder diffractometry (XRPD), flame atomic absorption spectroscopy (FAAS) and chemical analysis have been used.

Experimental Section

1. Starting chemicals and sample preparation

The starting chemicals were purchased from Aldrich Chimica (Italy): Fe_2O_3 (purity >99%), MnO (purity >99%) and Mn_3O_4 (purity 97%). Physical mixtures of composition (in molar ratio) $MnO-Fe_2O_3$ (1:1) and $Mn_3O_4-Fe_2O_3$ (1:3) were pre-

pared by weighing the appropriate amounts of the components and by mixing them in agate jars without milling media for 1 h at 100 rpm. The physical mixtures were dry milled for 130 h in a high energy planetary mill (Pulverisette 7 by Fritsch, Germany) at 350 rpm rotation speed with 3 agate balls (12 mm diameter) in agate jars. The ball/sample mass ratio was 5:1. After the allotted time the jars were opened and the samples were scraped from the jars: henceforth we will refer to these samples as milled or mechanically activated mixtures. Finally they were subjected to the thermal treatment described in the following.

2. Experimental techniques

- TGA measurements were performed with the 2950 thermogravimetric analyser (TA Instruments Inc. USA) connected to the TA5000 computer (also by TA Instruments Inc. USA). About 50 mg samples (both physical and milled mixtures) were placed in a Pt sample holder and heated at 5 K/min under a nitrogen flow of 100 ml/min at temperatures from 25 up to 600, 700, 800 and 900 °C. An isothermal stage of 12 h was appended at the end of the ramps. The physical and milled mixtures have also been subjected to the following thermal schedule (stepwise isothermal): about 50 mg samples were placed in a Pt sample holder and heated at 5 K/min under a nitrogen flow of 100 ml/min from 25 up to 200, 300, 400, 500, 600, 700, 800, and 900 °C with an isothermal stage of 5 h at each temperature.
- Some TG measurements were carried out on the milled mixture with the thermobalance (TGA 951 Thermogravimetric Analyser by DuPont Inc. USA) connected to an FT-IR spectrometer (Model 730 FT-IR by Nicolet USA equipped with OMNIC™ proprietary software). The sample was heated to 500 °C to analyse the gases evolved. Nitrogen was used both as purging gas (20 l/min) for the spectrometer and to sweep (65 ml/min) the gaseous products from the thermobalance into the FT-IR gas cell heated at 200 °C. The spectra of the evolved gases were obtained by fast Fourier transform of 16 coadded interferograms collected at 8 cm^{-1} resolution.
- X-ray diffraction patterns of the thermally treated samples were taken by putting the samples on a non-diffracting silicon slide. Use was made of an X-ray powder diffractometer (Bruker D5005) equipped with a goniometer and a graphite bent crystal monochromator. XRD patterns were recorded in step scan mode (Cu-K_α, 40 kV, 40 mA, step 0.02°, 3s/step, 2ϑ range 20–70°).
- About 1 g samples of the milled mixtures were heated in a tubular furnace (Carbolite MTF 12/38/400) at 5 K/min up to 900 °C and kept at this temperature for up to 8–12 h. The XRD patterns were recorded in step scan mode (Cu-K_α, 40 kV, 40 mA, step 0.02°, 5s/step , 2ϑ range 15–115°). From the XRD patterns the lattice parameters of the samples have been calculated by a least squares refinement procedure.
- The samples where only the presence of $MnFe_2O_4$ has been previously assessed were examined by DSC to check the Curie temperature. Measurements were performed (DSC 2920 by TA Instruments Inc. USA) at 10 K/min between 25 and 400 °C.
- The determination of the Mn content in the samples was made by flame atomic absorption spectroscopy (FAAS Perkin Elmer Model 1100B Flame Air Acetylene) following the manufacturer's instructions. Solid samples (about 80 – 100 ± 0.1 mg) were treated with 20 ml of 6 M HCl on a hot plate. The limpid solution was cooled to room temperature, diluted to a suitable volume and analyzed by FAAS for total Mn content.
- Chemical analyses. The content of Mn(III) in the samples has been determined as follows: solid samples (about 80 – 100 ± 0.1 mg) were treated with 10 ml of deionized water, 10 ml of 0.1 N Fe(II) standardized solution and 5 ml of 5 M H_2SO_4. In cases where the starting sample is pure Mn_3O_4, limpid solutions are obtained and excess Fe(II) is titrated with standardized 0.1 N $KMnO_4$. In the case of the mixtures with Fe_2O_3, the obtained suspension is filtered before titration with $KMnO_4$. The reactions taking place are: $MnO \cdot Mn_2O_3 + 8\ H^+ + 2\ Fe^{2+} \rightarrow 3\ Mn^{2+} + 2\ Fe^{3+} + 4\ H_2O$ and $MnO_4^- + 5\ Fe^{2+} + 8\ H^+ \rightarrow Mn^{2+} + 5\ Fe^{3+} + 4\ H_2O$. It has to be underlined that Mn(IV) also undergoes the first reaction (see comments in the text).

Results and Discussion

1. Mixture $MnO–Fe_2O_3$

Figure 1 reports the XRD patterns of the $MnO–Fe_2O_3$ milled mixture: the MnO peaks are barely visible as shoulders of those, rather broad, that are characteristic of Fe_2O_3. No other Mn compounds (oxides and/or carbonates) could be found

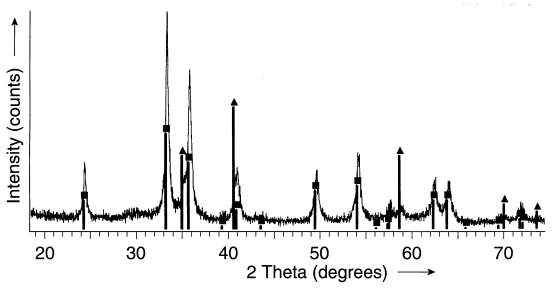

Fig. 1. XRDP patterns of the milled $MnO-Fe_2O_3$ mixture. ▲ MnO (JCPDS file n. 07-0230); ■ Fe_2O_3 (JCPDS file n. 33-0664)

by XRPD. A TG run at 10 K/min has been performed on the milled mixture where the evolved gas has been passed through a heated IR cell so that the real time IR spectra could be recorded. Figure 2 shows the IR spectra of the gaseous effluent released between 25 and 270 °C (a mass loss of −1.14% was recorded): it can be seen that CO_2 is the only gas evolved (peaks at ≈2350 and 670 cm^{-1}). This means that milling is likely to have caused the formation of some $MnCO_3$. By referring the mass loss recorded during the TG/IR measurements to the reaction:

$$MnCO_3\ (s) \rightarrow MnO\ (s) + CO_2\ (g) \qquad (1)$$

a $MnCO_3$ content of ≈3% by mass in the milled mixture can be calculated which lies below the detection limit of XRPD.

The effect of milling has been studied also on pure MnO milled for 100 h under the same conditions adopted for the $MnO-Fe_2O_3$ mixture. A TG experiment on milled MnO has been performed at 5 K/min (under N_2) up to 820 °C. After a minor mass loss (≈ −0.2%), the mass increases up to a constant value (ΔM = +4.9%). Despite the fact that the recorded mass increase is lower than that expected for complete $MnO \rightarrow Mn_3O_4$ oxidation (+7.5%), the XRD patterns of the sample recovered after the TG run only show the Mn_3O_4 reflexions meaning that partial $MnO \rightarrow Mn_3O_4$ oxidation occurred during milling (≈0.33 moles of MnO transform to Mn_3O_4 yielding ≈10% Mn_3O_4 by mass in the milled mixture). Hence both $MnCO_3$ formation and $MnO \rightarrow Mn_3O_4$ oxidation take place as a consequence of high energy milling.

Figure 3 shows the TGA curves obtained by heating the milled mixture under nitrogen at 5K/min up to different temperatures (600–700–800–900 °C + 12 h isothermal stage). Table 1 reports the data relevant to some points of the runs (reference to Fig. 3 should be made). The mass loss between the beginning of the run and ≈400 °C (T_{min}) is likely to be due to $MnCO_3$ decomposition. Since the mean value of M_{min} is 98.71%, a 3.4% of $MnCO_3$ by mass in the starting milled mixture is calculated which agrees fairly well with the ≈3% found in the TG/IR experiment. The mass loss between ≈600 °C (T_{max}) and the end of the runs increases with increasing the annealing temperature, and a constant mass value is reached at 900 °C.

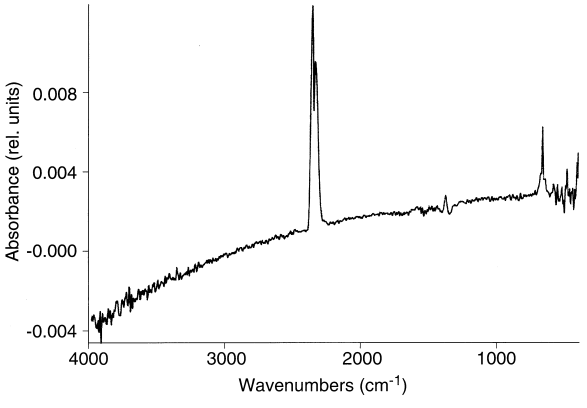

Fig. 2. IR spectrum of the gaseous effluent released between 25 and 270 °C from a sample of the milled $MnO-Fe_2O_3$ mixture (10 K/min, nitrogen flow).

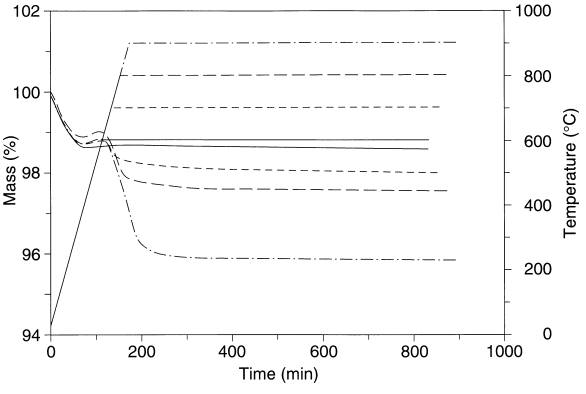

Fig. 3. TG curves of the milled $MnO-Fe_2O_3$ mixtures. The samples were heated to 600 °C (solid line), 700 °C (short-dashed line), 800 °C (long-dashed line), 900 °C (dash-dotted line). At each temperature a 12 h isothermal period was appended to the heating ramp.

T_{final}	M_{min} [%]	T_{min}	M_{max} [%]	T_{max}	$\Delta M_{max\text{-}fin}$ [%]
600	98.62	419.53	98.67	600	–0.09
700	98.71	387.45	98.79	589.34	–0.80
800	98.88	379.31	99.01	565.05	–1.47
900	98.61	417.36	98.68	606.99	–1.88
mean	98.71 ± 0.12		98.79 ± 0.16		

Table 1. TG measurements performed on the milled MnO–Fe_2O_3 mixture. T_{min} (°C) represents the temperature where the mass attains a relative minimum (M_{min}, %). T_{max} (°C) represents the temperature where the mass attains a relative maximum M_{max}(%). $\Delta M_{max\text{-}fin}$ (%) is the mass loss occurring between T_{max} and the end of the run.

The mass loss can be accounted for by the reaction:

$$(1/3)\ Mn_3O_4\ (s) + Fe_2O_3\ (s) \rightarrow MnFe_2O_4\ (s) + (1/6)\ O_2\ (g) \qquad (2)$$

This reaction takes place if MnO has been partially oxidized to Mn_3O_4 during milling as it was the case with pure MnO. Figure 4 shows that the sample, after its annealing at 600 °C, only shows the XRD peaks of Fe_2O_3, whereas the samples annealed at T > 600 °C also show the peaks of $MnFe_2O_4$ that are the only diffraction effects of the mixture annealed at 900 °C. This fact has been confirmed by taking the XRD patterns of a massive sample annealed at 900 °C under N_2 for 12 h in the furnace. The lattice constant of the obtained product is a = 8.5200 ± 0.0010 Å in fair agreement with that reported in the JCPDS file n. 10-0319. Furthermore a DSC run performed on this same sample showed a transition that corresponds to the Curie temperature (see Fig. 5 trace a). On the other hand, if all of MnO had been oxidized during milling, the mass loss of reaction (2) would be –2.28% instead of –1.88%. The lower than expected mass loss demonstrates that only 0.822 moles of MnO were oxidized to Mn_3O_4 during milling. However, the extent of MnO oxidation to Mn_3O_4 is sensibly higher when the milling is performed on the mixture with Fe_2O_3: such an enhanced "tribochemical" oxidation is likely to be due to the mechanical stress exerted on the softer (MnO) of the two phases as it could be observed in other cases [10]. The fact that the only product obtained at 900 °C is $MnFe_2O_4$, means that some reaction takes place also between MnO and Fe_2O_3 as it could be confirmed by the TG measurement performed with the stepwise isothermal schedule.

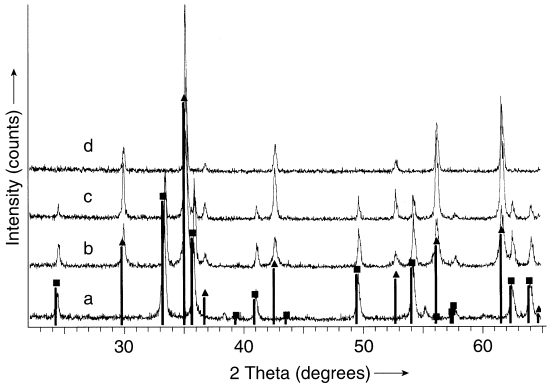

Fig. 4. XRDP patterns of the milled MnO–Fe_2O_3 mixtures recovered after 12 h isotherms at 600 °C (a), 700 °C (b), 800 °C (c) and 900 °C (d). ▲ $MnFe_2O_4$ (JCPDS file n. 10-0319); ■ Fe_2O_3 (JCPDS file n. 33-0664)

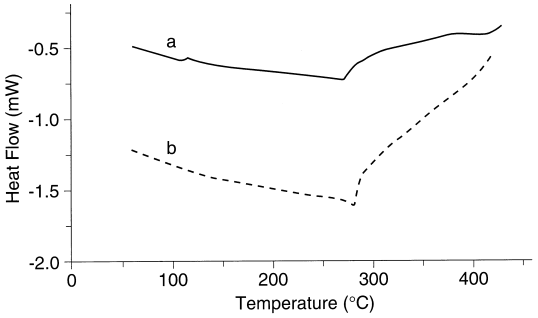

Fig. 5. DSC runs performed at 10 K/min on samples of milled (a) MnO–Fe_2O_3 and (b) (1:3)Mn_3O_4–Fe_2O_3 mixtures previously annealed (12 h 900 °C under N_2).

Table 2. TG measurements performed on the milled MnO–Fe_2O_3 mixture with the stepwise isothermal schedule. M_{init} and M_{fin} represent the initial and final mass values for each isothermal stage. ΔM_{iso} is the corresponding mass variation.

T_{iso} [°C]	M_{init} [%]	M_{fin} [%]	ΔM_{iso} [%]
200	99.02	99.05	+0.03
300	98.97	99.08	+0.11
400	99.08	99.20	+0.12
500	99.16	98.99	–0.17
600	98.88	98.72	–0.16
700	98.46	97.98	–0.48
800	97.78	97.29	–0.49
900	97.03	96.80	–0.23

Table 2 reports the mass values recorded at the beginning and at the end of each isothermal period. After $MnCO_3$ decomposition (step at 200 °C), a limited mass increase takes place at 300 and 400 °C whereas, from 500 °C, the mass begins to decrease until it reaches a constant value. The mass loss of −2.40% agrees fairly well with the value expected for complete formation of $MnFe_2O_4$ (confirmed by the XRPD patterns of the residue after the run) according to reaction (2). Clearly in this TG measurement enough time is allowed at 300–400 °C to complete MnO oxidation to Mn_3O_4.

Figure 6 shows the TGA curves obtained by heating the physical mixture under nitrogen up to different temperatures (600, 700, 800 and 900 °C + 12 h isothermal stage). The sample mass attains a final value (not constant at any temperature) that decreases with increasing the annealing temperature. The run up to 600 °C shows an increasing mass up to a value (102.32%) which corresponds to the oxidation of MnO to Mn_3O_4. Indeed the XRPD patterns of the residual sample only show the peaks of Fe_2O_3 and Mn_3O_4. The sample reacted at 700 °C shows a mass increase up to a value of 102.1%. Afterwards the mass slowly decreases to 102.0% but no constant mass is reached by the end of the run. The mass decrease after the maximum indicates that the reaction between Mn_3O_4 and Fe_2O_3 to give $MnFe_2O_4$ begins at about 700 °C. The XRPD patterns of the residual sample show, besides those of Mn_3O_4 and Fe_2O_3, the peaks of $MnFe_2O_4$. The sample reacted at 800 °C exhibits a mass increase up to a maximum (101.6%) which is lower than the maxima at the two lower temperatures (600 and 700 °C). After the maximum, the mass decreases to 101.4% and the XRD patterns of the residual sample show that the relative intensity of the peaks of Mn_3O_4 and Fe_2O_3 has decreased (with respect to the sample annealed at 700 °C) whereas the relative intensity of the $MnFe_2O_4$ peaks has increased. Clearly at this temperature the reaction between MnO and Fe_2O_3 is competing with MnO oxidation to give Mn_3O_4. The mass of the sample heated at 900 °C shows the same qualitative behaviour: the relative maximum (101.0%) is lower than that at 800 °C whereas the subsequent mass decrease is higher. The relative share of the reaction between MnO and Fe_2O_3 has increased with respect to that of the reaction between Mn_3O_4 and Fe_2O_3. The intensities of the peaks of $MnFe_2O_4$ are higher than at 800 °C though XRD evidence of unreacted Mn_3O_4 and Fe_2O_3 is still present. The course of the reaction in the case of the physical mixture is confirmed by the stepwise TG measurement. Table 3 reports the mass values recorded at the beginning and at the end of each isothermal period. The mass increases during each of the isothermal steps up to 600 °C and this confirms that the only reaction taking place in this temperature range is MnO oxidation to Mn_3O_4. The trend of the mass reverses during the isothermal stage at 700 °C: first the mass reaches a maximum value (102.20%) that nearly corresponds to the complete MnO oxidation to Mn_3O_4 and then it starts to decrease as reaction (2) gradually occurs. However in the case of the physical mixture the mass at the end of the

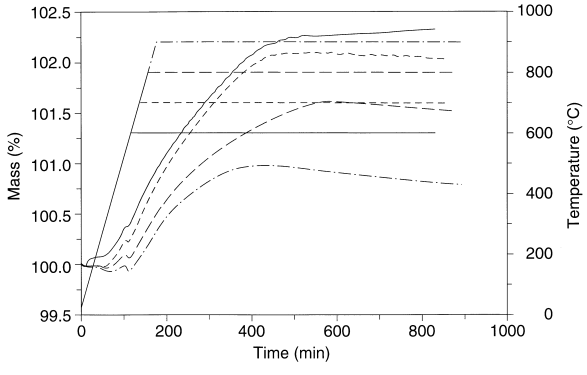

Fig. 6. TG curves of the physical mixture $MnO–Fe_2O_3$. The samples were heated to 600 °C (solid line), 700 °C (short-dashed line), 800 °C (long-dashed line), 900 °C (dash-dotted line). At each temperature a 12 h isothermal period was appended to the heating ramp.

Table 3. TG measurements performed on the physical $MnO–Fe_2O_3$ mixture with the stepwise isothermal schedule. M_{init} and M_{fin} represent the initial and final mass values. ΔM_{iso} is the corresponding mass variation.

T_{iso} [°C]	M_{init} [%]	M_{fin}(%)	ΔM_{iso} [%]
200	99.96	99.98	+0.02
300	99.98	100.20	+0.22
400	100.30	100.50	+0.20
500	100.50	101.10	+0.60
600	101.20	101.90	+0.70
700	102.00	102.10	+0.10
800	102.00	101.70	–0.30
900	101.50	101.00	–0.40

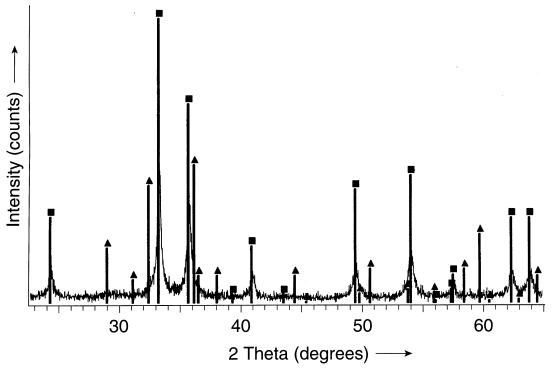

Fig. 7. XRDP patterns of the milled (1:3)Mn_3O_4–Fe_2O_3 mixture. ▲ Mn_3O_4 (JCPDS file n. 24-0734); ■ Fe_2O_3 (JCPDS file n. 33-0664).

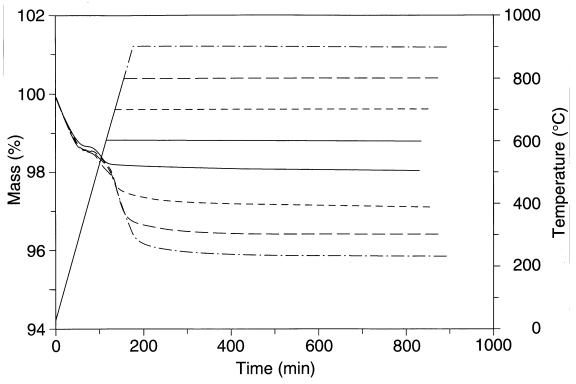

Fig. 8. TG curves of the milled (1:3)Mn_3O_4–Fe_2O_3 mixtures. The samples were heated to 600 °C (solid line), 700 °C (short-dashed line), 800 °C (long-dashed line), 900 °C (dash-dotted line). At each temperature a 12 h isothermal period was appended to the heating ramp.

5 h-isothermal stage at 900 °C is higher than the initial mass meaning that the formation of $MnFe_2O_4$ according to reaction (2) is far from complete (as confirmed by XRD patterns of the residual sample that show, besides those of $MnFe_2O_4$, also the reflexions of unreacted Fe_2O_3 and Mn_3O_4).

2. Mixture Mn_3O_4–Fe_2O_3

Figure 7 reports the XRD patterns of the (1:3) Mn_3O_4–Fe_2O_3 milled mixture: the Mn_3O_4 peaks have disappeared and only the Fe_2O_3 reflexions, rather broad, are present. The apparent absence of Mn_3O_4 in the milled mixture is due to a preferential amorphisation of the softer of the two phases (Mn_3O_4), which has been noted previously [10, 11]. Figure 8 shows the TGA curves obtained by heating the milled mixture under nitrogen up to different temperatures (600–700–800–900 °C + 12 isothermal stage). Table 4 reports the data relevant to some points of the run (reference to Fig. 8 should be made). The mass loss (ΔM_0) between the beginning of the run and ≈ 400 °C (T_0) has been shown by TG/IR to correspond to the release of both water and carbon dioxide. The mass loss between T_0 and the end of the run (ΔM_{HT+iso}) increases by increasing T_{iso} and, in the case of the sample annealed at 900 °C, sensibly exceeds the value expected for reaction (2). It has to be noted (see Fig. 9) that the residuals examined by XRPD only showed the Fe_2O_3 reflexions (600 °C) whereas, by annealing at 700 and 800 °C, also the peaks of $MnFe_2O_4$ are present. This is the only compound present after the annealing at 900 °C. This fact has been confirmed by taking the

Table 4. TG measurements performed on the milled Mn_3O_4–Fe_2O_3 mixture. ΔM_0 (%) is the mass loss occurring between 25 °C and T_0 (°C). ΔM_{HT+iso} is the mass loss between T_0 and the end of the run.

T_{iso} (°C)	ΔM_0	T_0	ΔM_{HT+iso}
600	–1.35	404	–0.61
700	–1.45	394	–1.44
800	–1.48	412	–2.07
900	–1.46	417	–2.68

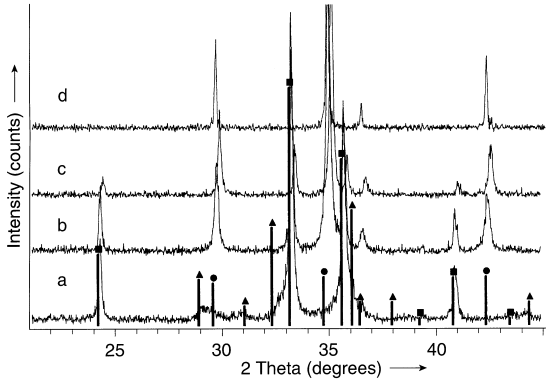

Fig. 9. XRDP patterns of the milled (1:3)Mn_3O_4–Fe_2O_3 mixtures recovered after 12 h isotherms at 600 °C (a), 700 °C (b), 800 °C (c) and 900 °C (d). ● $MnFe_2O_4$ (JCPDS file n. 10-0319); ▲ Mn_3O_4 (JCPDS file n. 24-0734); ■ Fe_2O_3 (JCPDS file n. 33-0664).

XRPD patterns of a massive sample annealed under N_2 at 900 °C for 12 h in the furnace. The lattice constant of the obtained product is 8.5106 ± 0.0020 Å which is in fair agreement with that reported in the JCPDS file n. 10-319 (8.499 Å). Furthermore a DSC run on this same sample showed a Curie temperature very close to that of the sample obtained by subjecting to the same thermal schedule a sample of the $MnO-Fe_2O_3$ milled mixture (see Fig. 5 trace b).

A more thorough TG examination of the milled mixture has been performed by heating-cooling (10K/min under N_2) a sample between 25 °C and 400 °C. This cycle has been followed by a heating up to 1200 °C. Such an experiment has been replicated four times. The mean value of the mass loss up to 400 °C is −1.53 ± 0.18%. During cooling to room temperature a mass gain of +0.36 ± 0.08% is recorded. The final heating shows two steps: the first one ends at ≈ 400 °C and involves a mass loss of −0.34 ± 0.02% whereas the second one shows a mass loss of −2.81 ± 0.09%. The fact that a share of the mass loss up to T_0 is reversible suggests it is due to oxygen loss/intake. Therefore the residual mass loss within T_0 ($\Delta M = -1.17 \pm 0.22\%$) is due to the release of the volatile impurities absorbed during milling. Again it is to note that the mass loss of −2.81% is higher than the value (−2.23%) expected for reaction (2). The reason for such a higher than expected mass loss could be hypothesized to be the presence of some Mn(III) in the milled sample. In this instance the reaction of $MnFe_2O_4$ formation would be:

$$(x/3)\,Mn_3O_4\,(s) + [(1-x)/2]\,Mn_2O_3\,(s) + Fe_2O_3\,(s) \rightarrow MnFe_2O_4\,(s) + [(3-x)/12]\,O_2\,(g) \quad (3)$$

From the mass loss of −2.81% the × value of 0.475 can be deduced. If this interpretation is correct the content of Mn(III) in the milled mixture would be 19.30% by mass instead of the expected 15.29%. Such an hypothesis has been confirmed by chemical analysis that yielded a Mn(III) content in the milled mixture of 19.7 ± 0.2% by mass. In Table 5 the calculated and experimental content (mean of 3 independent replicates) of Mn(III) and of total Mn both in pure Mn_3O_4 (milled and unmilled) and in (1/3)$Mn_3O_4-Fe_2O_3$ mixtures (milled and unmilled) is reported. However the analytical method employed involving titration of manganese with Fe(II), does not distinguish between Mn (III) and Mn (IV). Therefore the possibility that some Mn^{2+} was been oxidized to Mn (IV) [instead of Mn(III)] cannot be ruled out. If this were true, it could be that the formation of $MnFe_2O_4$ from the milled mixture is due to some catalytic effect exerted by Mn (IV) rather than to the mechanical activation of the mixture. To try and establish this point a mixture Mn_3O_4 (with 2.5% by mass of MnO_2)$-Fe_2O_3$ (Mn:Fe molar ratio 1:2 in the mixture) was prepared and heated at 5 K/min under N_2 up to 900 °C + 12 h isothermal stage. A mass loss of −1.53% (*vs.* expected −2.37%) was recorded that points to a catalytic effect of Mn(IV). It may well be that such a lower than expected mass loss is due to the fact that in this case Mn(IV) has been added deliberately whereas it would be gradually forming in the case of the milled mixtures so enhancing its homogeneous distribution and hence its catalytic effect. However, it should be noted that, to obtain complete formation of $MnFe_2O_4$ at 900 °C , the MnO_2-doped mixture had to be milled before being annealed at 900 °C (12 h, under N_2). Work is in progress to gather more information on this aspect.

The stepwise isothermal experiment was run also on this milled mixture. Within the isothermal stage at 300 °C the mass reaches the 98.7% of its initial value (due to loss of the volatile impurities). The second mass loss process begins at 400 °C and ends at 900 °C with a $\Delta M = -2.85\%$. Therefore the value found in the dynamic runs performed at 10K/min up to 1200 °C is confirmed.

The physical mixture was also heated under N_2 up to different temperatures (600–700–800–

Sample	Mn(III) (mass%) Expected	Found	Mn total (mass%) Expected	Found
Mn_3O_4 unmilled	48.0	49.0 ± 0.5	72.0	70.1 ± 0.5
Mn_3O_4 milled	48.0	50.2 ± 1.0	72.0	70.3 ± 0.4
(1:3)Mn_3O_4–Fe_2O_3 unmilled	15.3	16.3 ± 0.3	23.4	23.1 ± 0.3
(1:3)Mn_3O_4–Fe_2O_3 milled	15.3	19.7 ± 0.2	23.4	23.4 ± 0.3

Table 5. Calculated and experimental values (mean of 3 independent replicates) of Mn(III) and total Mn content (% by mass) both in pure Mn_3O_4 (milled and unmilled) and and in (1:3)Mn_3O_4–Fe_2O_3 mixtures (milled and unmilled).

900 °C + 12 h isothermal stage) : The TGA curves show that, apart from some minor mass fluctuations in the dynamic part of the run, there is no significant mass loss and , accordingly, the XRD patterns of the residual samples only show the reflexions of unreacted Mn_3O_4 and Fe_2O_3.

Conclusions

- Thermal treatment at 900 °C (under nitrogen) of a milled $MnO-Fe_2O_3$ mixture yields $MnFe_2O_4$ mainly as the product of the reaction between Mn_3O_4 (produced by ball milling) and Fe_2O_3. No complete transformation to $MnFe_2O_4$ is obtained (under the same experimental conditions) when starting from a $MnO-Fe_2O_3$ physical mixture.
- Thermal treatment at 900 °C (under nitrogen) of the milled $Mn_3O_4-Fe_2O_3$ mixture yields $MnFe_2O_4$ mainly as the product of the reaction between Mn_3O_4 and Mn_2O_3/MnO_2 (produced by ball milling) and Fe_2O_3. The effect of high energy milling is more pronounced in this case than with the $MnO-Fe_2O_3$ mixture. Indeed no $MnFe_2O_4$ formation is obtained (under the same experimental conditions) when starting from a $Mn_3O_4-Fe_2O_3$ physical mixture.

[1] H. K. Harold, C. K. Mayfair, Adv. Catal. **33**, 159 (1985); R. R. Rajaram, A. Sermon, J. Chem. Soc. Faraday Trans. **181**, 2577 (1985); H. M. Cota, J. Katan, M. Chin, F. J. Schoenweis, Nature **203**, 1281 (1964); J. R. Goldstein, A. C. C. Tseung, J. Catal. **32**, 452 (1974); G. R. Dube, V. S. Darshane, Bull. Chem. Soc. Jpn. **64**, 2449 (1991).
[2] T. Kodama, M. Ookubo, S. Miura, Y. Kitayama, Mater. Res. Bull. **31**, 1501 (1996).
[3] H. Robbins, Ferrites, Proceedings of the 3th ICF Meeting, p. 70, Japan (1980).
[4] A. Rousset, Solid State Ionics **63–65**, 236 (1993).
[5] G. Bonsdorf, M. A. Denecke, K. Schäfer, S. Christen, H. Langbein, W. Gunser, Solid State Ionics, **101–103**, 351 (1997).
[6] N. M. Deraz, G. A. El-Shokabi, Thermochim. Acta **375**, 137 (2001).
[7] V. Berbenni, A. Marini, N. J. Welham, P. Matteazzi, N. Ricceri, J. Eur. Cer. Soc. **23**, 529 (2002).
[8] V. Berbenni, A. Marini, N. J. Welham, P. Galinetto, M. C. Mozzati, J. Eur. Cer. Soc. **23**, 179 (2002).
[9] V. Berbenni, A. Marini, Mater. Res. Bull. **37**, 221 (2002).
[10] N. J. Welham, Mater. Sci. Eng. A, **255**, 81 (1998).
[11] A. W. Weeber, H. Bakker, Physica B, **153**, 93 (1988).